



DRX rules during extrusion process of large-scale thick-walled Inconel 625 pipe by FE method

Li DANG¹, He YANG¹, Liang-gang GUO¹, Lei SHI¹, Jun ZHANG², Wen-da ZHENG²

1. State Key Laboratory of Solidification Processing, Northwestern Polytechnical University, Xi'an 710072, China;
2. China National Heavy Machinery Research Institute Corporation, Xi'an 710032, China

Received 17 November 2014; accepted 20 January 2015

Abstract: A thermal-mechanical and micro-macro coupled finite element (FE) model for the hot extrusion process of large-scale thick-walled Inconel 625 pipe was developed based on the DEFORM-2D platform. Then, the influence rules of the key extrusion parameters on the average grain size and grain uniformity of the extruded pipe were revealed. The results show that with the increase of initial billet temperature, extrusion speed and friction coefficient, the grain uniformity is firstly improved and then deteriorated. Larger extrusion ratio leads to more uniform grain distribution. With the increase of initial billet temperature, the average grain size of the pipe first decreases and then increases. Additionally, larger extrusion ratio can bring smaller average grain size. The extrusion speed and friction coefficient have slight effects on the average grain size of the extruded pipe.

Key words: Inconel 625 alloy; large-scale thick-walled pipe; extrusion; dynamic recrystallization; grain size; grain uniformity

1 Introduction

Because of preferable heat resistance, agreeable strength, high ductility, favorable fatigue and corrosion resistance of Inconel 625 super alloy, large-scale thick-walled pipes made from it are widely used in many domains such as oil and chemical industry, thermal power generation, nuclear power plant, aerospace and defense industry [1–3]. In general, these pipes can be manufactured by many technologies such as rolling, spinning, forging and extrusion without remnant materials (EWRM). However, the EWRM process has become an irreplaceable forming technology for the manufacturing of large-scale thick-walled pipes due to some advantages such as obtaining finer microstructure, lower production cost, higher production efficiency and material utilization ratio.

The microstructure evolution of Inconel 625 alloy has been studied by many researchers through isothermal compression and torsion tests [4–7]. The results show that the dynamic recrystallization (DRX) is a key mechanism of microstructure transformation and is mainly affected by temperature, strain and strain rate. At

the same time, the DRX model of this alloy is also developed by WU et al [6], which provides an important foundation for the microstructure prediction of the deformed parts.

In addition, Inconel 625 is a single-phase austenite superalloy, so it is difficult to refine grains of this alloy by heat treatment. However, in view of the lower stacking fault of Inconel 625, DRX is highly probable to occur in hot plastic forming process and leads to grain refinement. Therefore, exploring the DRX rules under the key extrusion parameters, such as initial billet temperature (T_b), extrusion speed (v), extrusion ratio (λ) and friction coefficient (μ), is very useful for the optimal design and steady control of the extrusion process in terms of the microstructure of the extruded pipe.

For the microstructure of the extruded superalloy pipe, PENG et al [8] and WANG [9] experimentally studied the non-uniform distribution characteristics of grains along the thickness and length direction of the extruded GH690 pipe. GUO et al [10] studied the grain distribution in the extruded Inconel 625 pipe, which was non-uniform as well. In their research, the grain distribution characteristic of the extruded pipe was analyzed, but the influence rules of the key extrusion

Foundation item: Project (2009ZX04005-031-11) supported by the Major National Science and Technology Special Project of China; Project (KP200911) supported by the Research Fund of State Key Laboratory of Solidification Processing of China; Project (B08040) supported by the “111” Project of China

Corresponding author: He YANG; Tel/Fax: +86-29-88495632; E-mail: yanghe@nwpu.edu.cn
DOI: 10.1016/S1003-6326(15)63931-0

parameters, such as T_b , v , μ and λ , on the microstructure evolution of the pipe in the extrusion process were not discussed in detail. LIU et al [11] studied the effect of extrusion deformation on the grain size of FGH 96 alloy solution-treated at different temperatures, but the influence rules of extrusion parameters on the grain size were not discussed. GUO et al [12] studied the effects of initial billet temperature and extrusion speed on the DRX behavior of 304 stainless steel pipe during the extrusion process. From above analyses, researches on the DRX behavior of Inconel 625 pipe in the extrusion process are still lacking. Therefore, it is necessary to reveal the influence rules of key parameters on the DRX behavior of large-scale thick-walled Inconel 625 pipe in extrusion process for effective control of the pipes' microstructure.

However, it is wasteful and inefficient to reveal the influence rules of the key extrusion parameters by experiments due to high cost and the complexity in obtaining the microstructure of pipes. The finite element (FE) method is an efficient and economical alternative [12–14]. Therefore, in this work, a thermal-mechanical finite element model combined with the DRX model of Inconel 625 alloy was firstly developed for the extrusion process of large-scale thick-walled pipe. And then, on the basis of the FE model, the influence rules of the key extrusion parameters on the DRX behavior of the large-scale thick-walled Inconel 625 pipe were revealed.

2 Development of thermal-mechanical and micro-macro FE model

2.1 Geometrical model and mesh design

Figure 1 shows the EWRM principle of large-scale thick-walled Inconel 625 pipe and the die structure diagram. In the extrusion process, the extrusion pad, which is usually made from low alloy steel with lower deformation resistance, deforms when the pipe is

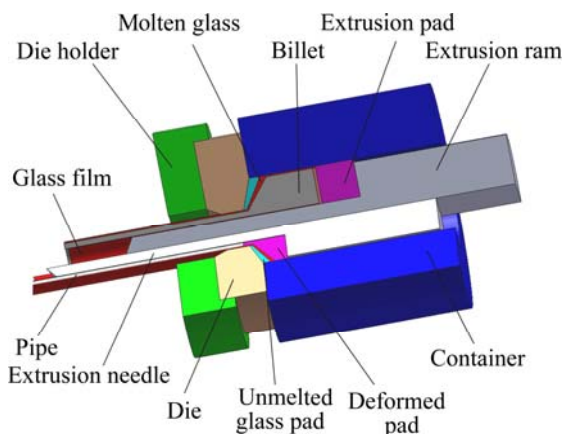


Fig. 1 Extrusion principle of extrusion without remnant materials process

completely extruded. Thus, the whole extruded pipe can be pushed out by the deformed extrusion pad. This extrusion process can improve not only the production efficiency, but also the material utilization ratio.

In current study, considering the symmetric geometry of the billet and extruded pipe, a 2D axisymmetric FE model for the process was established. Because of the same moving speed between extrusion needle and extrusion pad in the extrusion process, the ram shown in Fig. 2(a) was used to describe the geometries of the extrusion pad and the extrusion needle. On the other hand, the extrusion die and the container were fixed and contacted with each other in a practical extrusion process. Thus, the die shown in Fig. 2(a) was used to represent the geometries of the container and bottom die. In addition, in order to balance the simulation accuracy and efficiency, the mesh refinement is necessary in the main deformed region (see Fig. 2(b)), and the mesh design method was described and verified in Ref. [15], which is reasonable and acceptable.

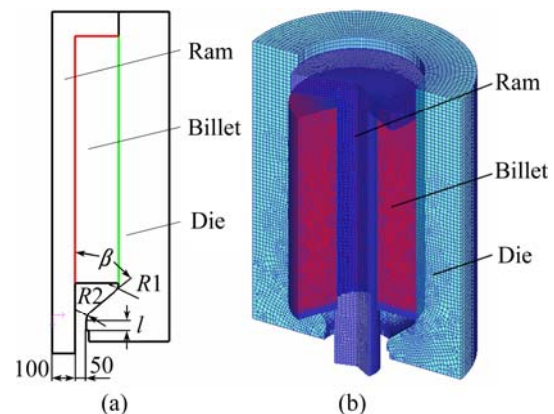


Fig. 2 2D axisymmetric geometrical model (a) and mesh design (b) of FE model

2.2 DRX evolution model

As mentioned above, the DRX is a key microstructure evolution mechanism of Inconel 625 alloy in the hot deformation process. In Ref. [6], the DRX evolution behavior of this alloy in the hot deformation process was studied through the isothermal compression experiments, and the dimensions of the experimental samples were $d8 \text{ mm} \times 12 \text{ mm}$. At the same time, the DRX evolution models were also developed, which are expressed by Eqs. (1)–(6). And Eq. (7) is the constructive equation of Inconel 625 obtained from Ref. [16]. In the equations, Z is the Zener–Hollomon parameter which is a function of temperature and strain rate; $\dot{\epsilon}$ is the strain rate (s^{-1}); ϵ_c is the critical strain for DRX; R is the mole gas constant ($R=8.314 \text{ J}/(\text{mol}\cdot\text{K})$); T is the deformation temperature (K); ϵ is the effective strain; d_0 is the initial grain size of billet (μm); X_{DRX} is the volume fraction of DRX grains; d_{DRX} is the DRX

gain size; $\varepsilon_{0.5}$ represents the strain when 50% of material experiences DRX; d is the grain size after DRX and σ_p is the peak stress. According to the results in Ref. [6], the values of X_{DRX} and d_{DRX} predicted by these models agree well with the experimental results, which verifies the DRX models:

$$Z = \dot{\varepsilon} \exp\left(\frac{635380}{RT}\right) \quad (1)$$

$$\varepsilon_c = \exp\left(-4.43 + 0.119 \ln \dot{\varepsilon} + \frac{2500}{T}\right) \quad (2)$$

$$\varepsilon_{0.5} = 0.00421Z^{0.11} \quad (3)$$

$$X_{\text{DRX}} = 1 - \exp\left(-1.22 \left(\frac{\varepsilon - \varepsilon_c}{\varepsilon_{0.5}}\right)^{2.5}\right) \quad (4)$$

$$d_{\text{DRX}} = \exp[(67.18 - \lg Z)/5.88] \quad (5)$$

$$d = d_0(1 - X) + d_{\text{DRX}}X \quad (6)$$

$$\dot{\varepsilon} = 0.45\sigma_p^{6.34} \exp\left(-\frac{401480}{RT}\right) \quad (7)$$

2.3 Thermal-mechanical and macro-micro coupled FE model and verification

In Ref. [10], the Inconel 625 pipe with dimensions of $d69.4 \text{ mm} \times 12.3 \text{ mm}$ was extruded under the conditions of $v=40 \text{ mm/s}$, $T_b=1473 \text{ K}$ and $\lambda=4.1$. At the same time, the grain distribution characteristics at top, middle and tail of the extruded pipe were analyzed. Therefore, in this section, the extrusion process of Inconel 625 pipe was simulated under the condition of $v=40 \text{ mm/s}$, $T_b=1473 \text{ K}$ and $\lambda=4.1$. The initial grain size of the billet, d_0 was set as $120 \mu\text{m}$ [10].

In addition, because the DRX evolution of Inconel 625 is sensitive to the deformation temperature [4, 5], the heat loss (including the emissivity and heat convection) of the billet when transferred from the furnace to the extruder was considered in the present FE model. The transferring time was 60 s, the heat conversion coefficient between billet and air was set as $20 \text{ W}/(\text{m}^2\cdot\text{K})$, the emissivity coefficient was 0.7. In the glass lubricated extrusion process, the heat transform coefficient and friction coefficient between billet and extrusion tools were set as $1500 \text{ W}/(\text{m}^2\cdot\text{K})$ and 0.02, respectively. In summary, the required simulation condition for the reliability evaluation of the DRX coupled FE model is shown in Table 1 [10, 17–19].

The DRX model and the constitutive model of the Inconel 625 alloy were encoded into the DEFORM-2D platform by the FORTRAN language. Subsequently, the required simulation conditions, which are shown in Table 1, were set in the pre-processor of DEFORM-2D, and the thermal-mechanical and macro-micro coupled FE model for Inconel 625 pipe extrusion process was developed.

Moreover, the calculation procedure of the Inconel 625 pipe extrusion considering DRX related microstructure evolution is shown in Fig. 3.

Table 1 Extrusion parameters setting for reliability evaluation of FE model [10,17–19]

Parameter	Value
Pipe size/mm	$d 69.4 \times 12.3$
Initial grain size/ μm	120
Transferring time of billet from furnace to extruder/s	60
Initial billet temperature/K	1473
Initial die temperature/K	573
Extrusion ratio	4.1
Die taper angle/ $^\circ$	75
Extrusion speed/ $(\text{mm}\cdot\text{s}^{-1})$	40
Heat convection coefficient between billet and air/ $(\text{W}\cdot\text{m}^{-2}\cdot\text{K}^{-1})$	20
Thermal emissivity of billet	0.7
Coulomb friction coefficient	0.02
Heat transform coefficient between billet and extrusion tool/ $(\text{W}\cdot\text{m}^{-2}\cdot\text{K}^{-1})$	1500

Figure 4 shows the experimental billet and the billet temperature distribution after the heat loss. It can be seen that the billet temperature decreases due to the heat convection and heat emissivity. The lowest temperature is at the corner of the billet. The temperature on the outer surface of the billet is lower than that on the inner surface of the billet due to larger heat radiation area of the outer surface.

Figure 5 shows the distribution of grain size after DRX, DRX volume fraction and DRX grain size of the simulated pipe. Figure 5(a) shows the grain distribution of the simulated pipe. It can be seen that the grain size at the tail and top of the simulated pipe is larger than that at other places due to lower DRX volume fraction and smaller DRX grain (Figs. 5(b) and (c)) caused by smaller deformation degree and lower deformation temperature.

In addition, the grain distribution in the middle of the extruded pipe was also analyzed in Ref. [10]. And the position of the observed sample points in the middle of the extruded pipe is shown in Fig. 6. Point *A* is about 1 mm from the inner surface of the pipe, point *B* is in the middle of pipe thickness, point *C* is about 1mm from outer surface of the pipe. The samples were etched with the corrosive comprising 10 mL H_2SO_4 , 100 mL HCl and 10 g CuSO_4 after grinding, and the grain distribution at points *A*, *B* and *C* is obtained through the Axiovert 200MAT optical microscope, which is shown in Fig. 7 [10].

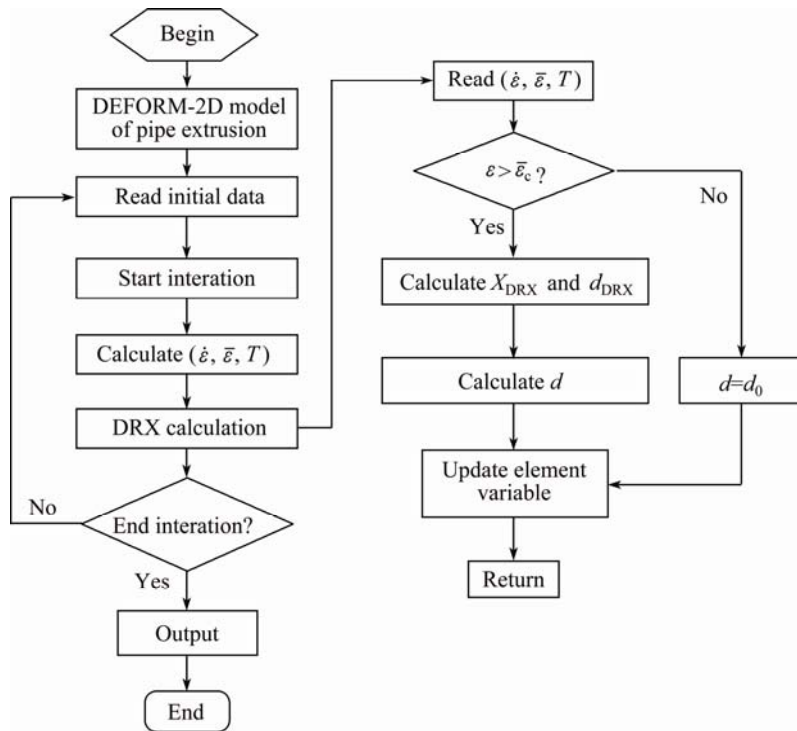


Fig. 3 Flow chart of DEFORM-2D FE simulation considering DRX microstructure evolution

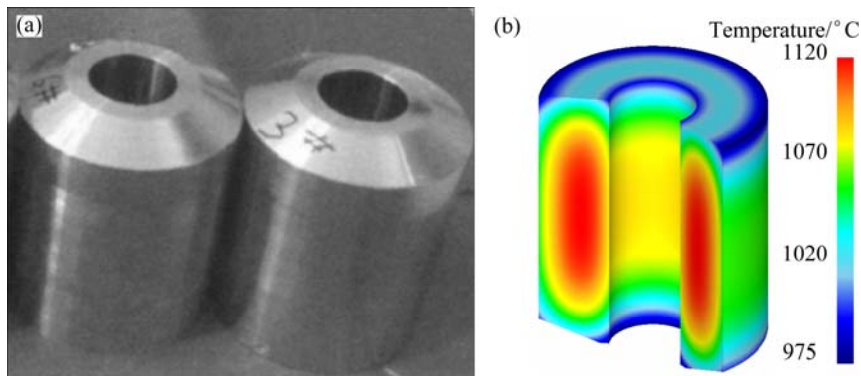


Fig. 4 Experimental billet (a) [10] and billet temperature distribution (b) before extrusion

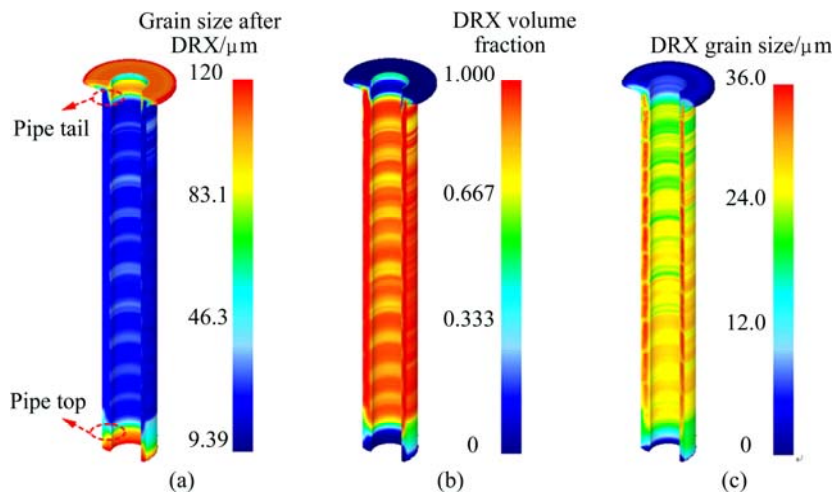


Fig. 5 Distribution of microstructure-related parameters calculated with established FE model: (a) Grain size after DRX; (b) DRX volume fraction; (c) DRX grain size

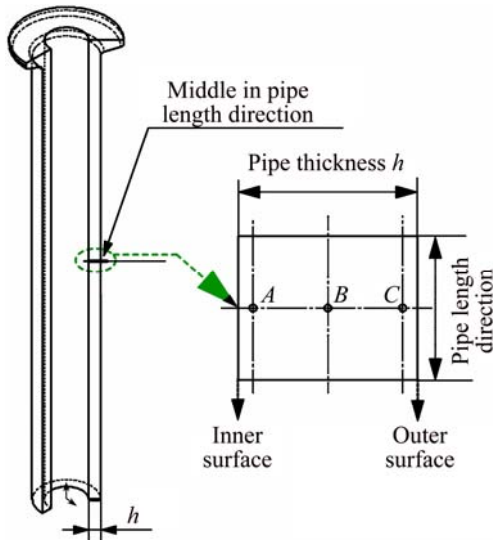


Fig. 6 Selection method of sample points for microstructure observation along pipe thickness direction in middle of pipe length

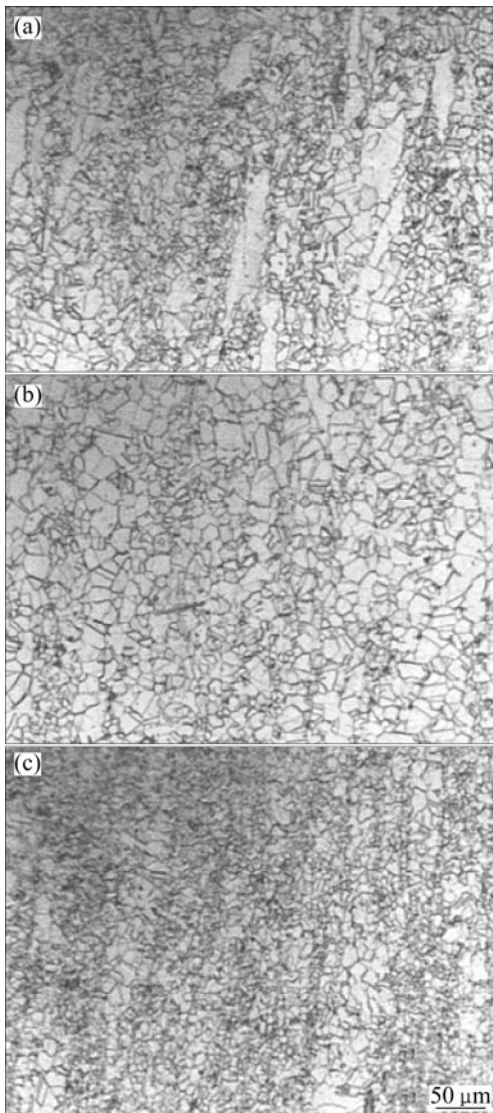


Fig. 7 Grain distribution in middle of extruded pipe at different positions [10]: (a) Point A; (b) Point B; (c) Point C

In addition, 50 grains were randomly selected in Figs. 7(a)–(c) to calculate the average grain size at points A, B and C. At the same time, for obtaining the grain size of the sample at points A, B and C on the simulated pipe, five sample points were selected near points A, B and C. The method to select the five points is shown in Fig. 8, and the average value of the five points is used to represent the simulated grain size of points A, B and C.

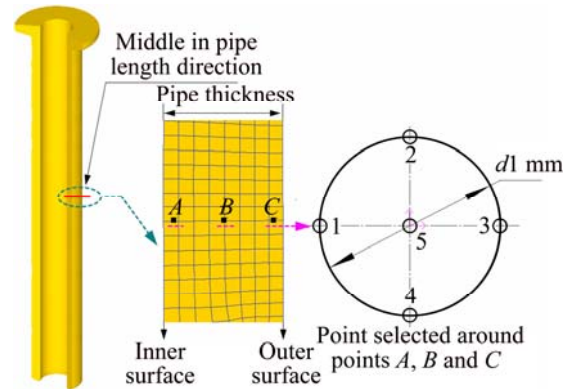


Fig. 8 Selection method of statistical points around points A, B and C for obtaining grain size of simulated pipe

Figure 9 shows the comparison of the simulated grain sizes with the experimental results in the middle of the pipe. It can be seen that the simulated grain size decreases from inside to outside of the pipe, the tendency agrees well with the experimental observation. In addition, the relative errors between the simulated and experimental results are $\delta_A=8.13\%$, $\delta_B=9.3\%$ and $\delta_C=15.56\%$, respectively, at points of A, B and C.

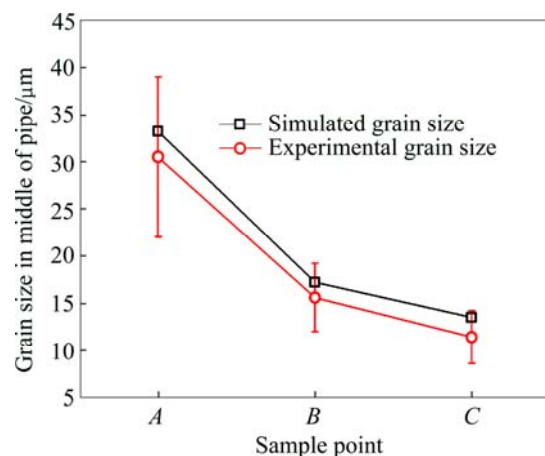


Fig. 9 Comparison between simulated grain size and experimental grain size

From the above analyses, the simulated grain distribution characteristics in the middle of the pipe are the same as the experimental observations. And the average error is 10.997%. This indicates that the FE model developed in this work can accurately describe the

DRX behavior of Inconel 625 pipe during the hot extrusion process.

3 DRX evolution of pipe in extrusion process

In the above section, the thermal-mechanical and micro-macro coupled FE model for the extrusion process of Inconel 625 pipe was developed. And in this section, the DRX evolution behavior of the large-scale thick-walled Inconel 625 pipe during the extrusion process was revealed based on this FE model. For this purpose, the simulation conditions shown in Table 2 [15,18,19] were used.

Figure 10 shows the grain size distribution of the pipe at different extrusion stages. It can be seen that the

Table 2 Extrusion parameters revealing DRX behavior of large-scale thick-walled Inconel 625 pipe during extrusion process [15,18,19]

Parameter	Value
Pipe size/mm	$d300 \times 50$
Initial grain size/ μm	120
Transferring time of billet from furnace to extruder/s	60
Initial billet temperature/K	1373
Initial die temperature/K	573
Extrusion ratio	5
Extrusion speed/($\text{mm} \cdot \text{s}^{-1}$)	150
Thermal emissivity of billet	0.7
Coulomb friction coefficient	0.02
Heat convection coefficient between billet and air/($\text{W} \cdot \text{m}^{-2} \cdot \text{K}^{-1}$)	20
Heat transform coefficient between billet and extrusion tool/($\text{W} \cdot \text{m}^{-2} \cdot \text{K}^{-1}$)	1500

grain size of the pipe becomes smaller when the billet is extruded through the die orifice due to the occurrence of DRX. And it can be seen from Fig. 10(e) that there is a coarse grain area at the top and tail of the pipe due to the smaller deformation degree and lower deformation temperature (see Figs. 11(a) and (b)) which can result in a smaller DRX degree (see Figs. 11(c) and (d)).

In addition, it can also be seen from Fig. 10(e) that the grain size in the inner layer of the pipe extruded at the stable stage gradually increases from top to the tail. The reason for this is the continuous decrease of the deformation temperature in the extrusion process (see Fig. 11(b)), which can result in a continuous decrease of the DRX volume fraction (see Fig. 11(c)) and DRX grain size (see Fig. 11(d)). Furthermore, it can also be seen that from Fig. 11(a) the effective strain of the pipe extruded in the stable stage has a slight change due to the unchanged extrusion ratio and constant extrusion speed in the extrusion process. So, it can be found from the above analysis that the deformation temperature is the main factor influencing the microstructure distribution of the extruded pipe.

4 Effects of key extrusion parameters on DRX evolution behavior

The DRX evolution behavior in the extrusion process was analyzed in the above sections. It can be found that there is a coarse grain area at the top and tail of the pipe, respectively, due to the lower DRX degree caused by the lower temperature and smaller deformation degree. And the coarse grain area will generally be removed in a practical application. Therefore, the pipe extruded in the stable stage was set as the research object in this section, and the effects of the key extrusion parameters on the average DRX volume fraction,

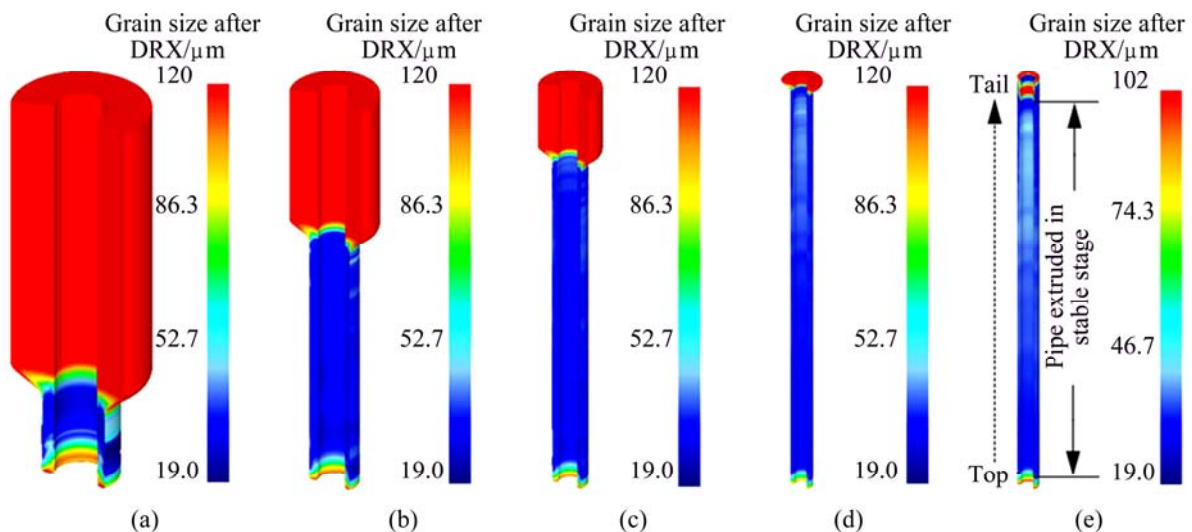


Fig. 10 Grain size distribution after DRX of pipe at different extrusion stages: (a) Step 300; (b) Step 900; (c) Step 1500; (d) Step 2100; (e) Step 2500

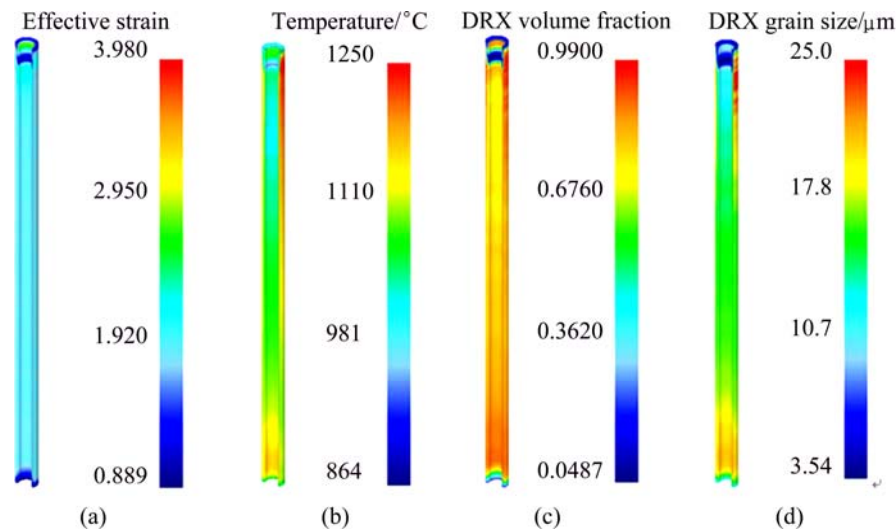


Fig. 11 Distribution of effective strain (a), temperature (b), DRX volume fraction (c) and DRX grain size (d)

average DRX grain size, average grain size and grain uniformity of the pipe extruded in stable stage were analyzed.

4.1 Simulation conditions and evaluation indicator

4.1.1 Simulation conditions

According to the reasonable range of the key extrusion parameters including T_b , v , λ and μ mentioned in Ref. [15], the following calculation conditions were used in this work for revealing the influence rules of the key extrusion parameters on the DRX evolution behavior of pipe extruded in the stable stage.

1) In order to reveal the influence rule of T_b on the DRX evolution behavior of the extruded Inconel 625 pipe, $v=150$ mm/s, $\lambda=6$ and $\mu=0.02$ were chosen, T_b was set as 1273, 1323, 1373, 1423 and 1573 K, respectively, but other parameters were retained as listed in Table 2, then five valid 2D-FE models for hot extrusion process of large-scale thick-walled Inconel 625 pipe were developed.

2) For revealing the influence rule of v on the DRX evolution behavior of the extruded Inconel 625 pipe, $T_b=1373$ K, $\lambda=6$ and $\mu=0.02$ were chosen, v was set as 100, 125, 150, 175 and 200 mm/s, respectively, but other parameters were retained as listed in Table 2, then five valid 2D-FE models for hot extrusion process of large-scale thick-walled Inconel 625 pipe were developed.

3) In order to reveal the influence rule of λ on the DRX evolution behavior of the extruded Inconel 625 pipe, $v=150$ mm/s, $T_b=1373$ K and $\mu=0.02$ were chosen, λ was set as 4, 5, 6 and 7, respectively, but other parameters were retained as listed in Table 2, then four valid 2D-FE models for hot extrusion process of large-scale thick-walled Inconel 625 pipe were developed.

4) For revealing the influence rule of μ on the DRX

evolution behavior of the extruded Inconel 625 pipe, $v=150$ mm/s, $\lambda=6$ and $T_b=1373$ K were chosen, μ was set as 0.01, 0.015, 0.02 and 0.025, respectively, but other parameters were remained as listed in Table 2, then four valid 2D-FE models for hot extrusion process of large-scale thick-walled Inconel 625 pipe were developed.

4.1.2 Evaluation indicator

In order to obtain the DRX grain size, DRX volume fraction and grain size after DRX of the pipe extruded in the stable stage, these values along the pipes' thickness direction but at different positions in the pipes' length direction were used (see Fig.12). And then, ten points with even distance were selected on each position (see Fig.12). So, a total of 50 sample points were selected for each pipe. Also, parameter d_{avg} described as Eq. (8) was used to evaluate the values of DRX grain size, DRX volume fraction and grain size of the pipe extruded in stable stage. The standard deviation (σ) of the grain size expressed as Eq. (9) was used to evaluate the grain

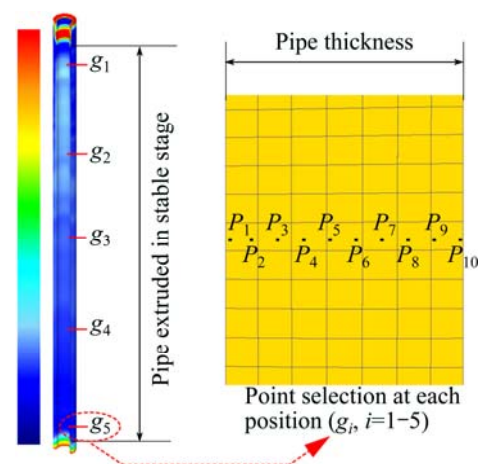


Fig. 12 Selection of sample points for obtaining grain size of simulated pipe extruded in stable stage

uniformity of the pipe extruded in stable stage. The larger σ indicates the worse grain distribution. In Eqs. (8) and (9), n is the number of the total sample points, x_i is the grain size after DRX of the i th point.

$$d_{\text{avg}} = \sum_{i=1}^n x_i / n \quad (8)$$

$$\sigma = \sqrt{\frac{\sum_{i=1}^n (x_i - d_{\text{avg}})^2}{n-1}} \quad (9)$$

4.2 Effects of key extrusion parameters

4.2.1 Initial billet temperature

Figure 13(a) shows the effect of initial billet temperature on the average DRX grain size and average DRX volume fraction of the pipe extruded in stable stage. It can be seen that the average DRX grain size and the average DRX volume fraction of the pipe increase with the increase of initial billet temperature. The reason for this can be that a higher deformation temperature of Inconel 625 can improve the DRX degree and increase the DRX grain size [4,5].

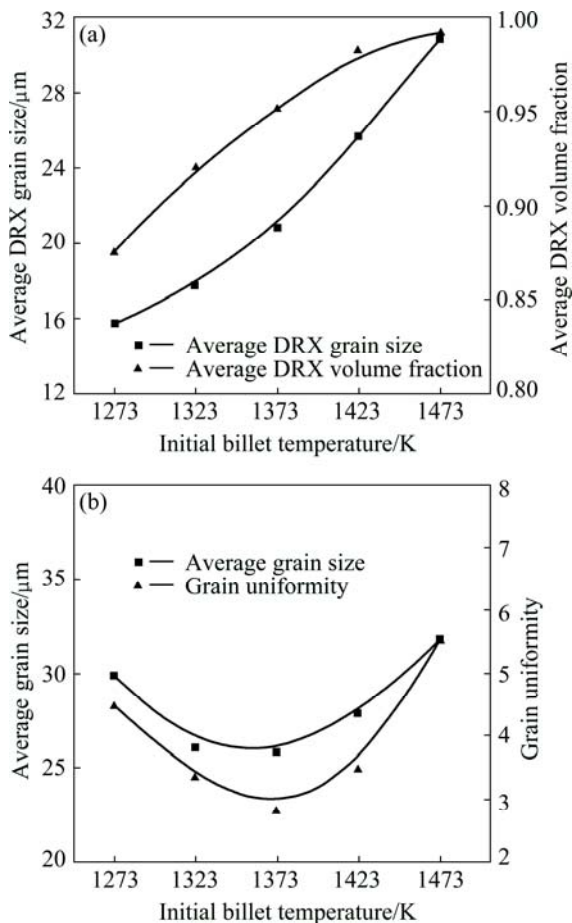


Fig. 13 Effect of initial billet temperature on DRX behavior in large-scale thick-walled Inconel 625 pipe extruded in stable stage: (a) Average DRX grain size and average DRX volume fraction; (b) Average grain size and grain uniformity

It can be seen from Fig. 13(b) that the average grain size of the pipe extruded in stable stage firstly decreases and then increases with the increase of initial billet temperature. The reason for this phenomenon can be explained by the fact that the incompleting DRX grains exist when the pipe is extruded under a lower initial billet temperature due to the lower DRX volume fraction. With the increase of initial billet temperature, the DRX grain size and DRX volume fraction increase continuously, which can decrease the volume fraction of the original grains, and then decrease the average grain size of the pipe. When the initial billet temperature becomes higher, the completed DRX grain can be obtained. So, the DRX grain grows larger at higher deformation temperature, and the average grain size of the pipe becomes larger.

In addition, the grain uniformity of the pipe extruded in stable stage firstly becomes better and then goes worse with the increase of initial billet temperature (see Fig. 13(b)). This phenomenon can be explained by that the uniformity of exit temperature in the extrusion process, which has a significant influence on the microstructure uniformity of the pipe, first becomes better and then goes worse with increasing initial billet temperature [15]. Furthermore, it can also be seen from Fig. 13(b) that the pipe with finer and more uniform grain can be obtained when the pipe is extruded at T_b of 1323–1423 K.

4.2.2 Extrusion speed

Figure 14(a) shows the effect of extrusion speed on the average DRX volume fraction and the average DRX grain size of the pipe. It can be seen that increasing extrusion speed can improve the average DRX volume fraction and increase the average DRX grain size of the pipe. The reason for this is that the increase of extrusion speed can induce more deformation heat and less heat loss of the billet, which can result in the increase of deformation temperature of the billet. So, the average DRX volume fraction and the average DRX grain increase with increasing the extrusion speed.

Figure 14(b) shows the effect of extrusion speed on the average grain size and grain uniformity. It can be found that the average grain size of the pipe has a slight decrease with the increase of extrusion speed.

The grain uniformity of the pipe firstly becomes better and then goes worse with increasing the extrusion speed. This can be attributed to that the exit temperature uniformity, which is the key factor influencing the microstructure uniformity of the pipe, firstly becomes better and then goes worse with increasing extrusion speed [15]. At the same time, it can also be seen from Fig. 14(b) that the grain distribution of the pipe will be

more uniform when the extrusion speed is in the range of 125–150 mm/s.

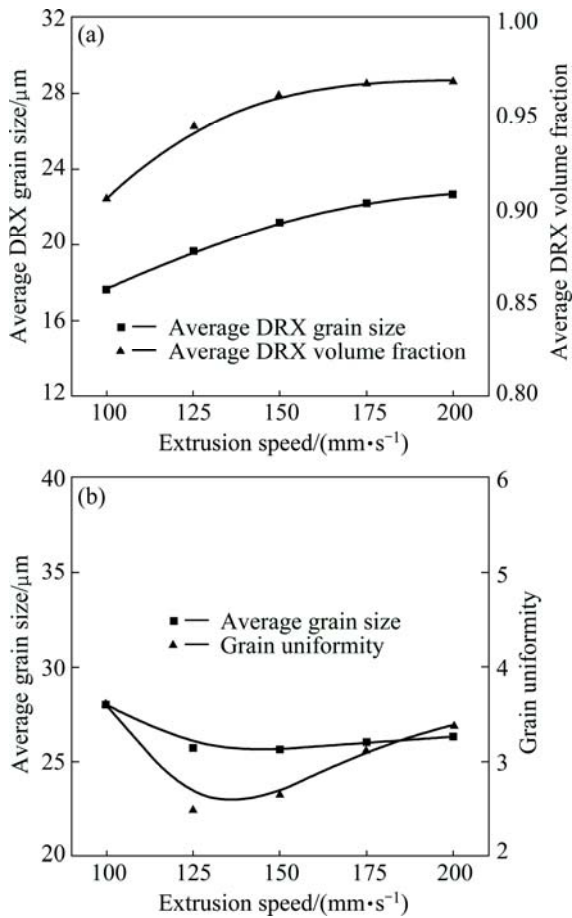


Fig. 14 Effect of extrusion speed on DRX behavior in large-scale thick-walled Inconel 625 pipe extruded in stable stage: (a) Average DRX grain size and average DRX volume fraction; (b) Average grain size and grain uniformity

4.2.3 Extrusion ratio

Figure 15(a) shows the effect of extrusion ratio on the average DRX volume fraction and average DRX grain size of the pipe extruded in stable stage. It can be seen that larger extrusion ratio can induce higher average DRX volume fraction and larger average DRX grain size. The reason for this can be that the larger extrusion ratio can induce larger deformation degree and more deformation heat, which can enhance the DRX degree and increase the DRX grain size of Inconel 625 pipe.

It can be seen from Fig. 15(b) that the average grain size of the pipe becomes smaller with the increase of extrusion ratio. The reason for this is that larger extrusion ratio can induce a larger deformation degree which can improve the DRX degree of the pipe. In addition, Fig. 15(b) also shows that the grain uniformity becomes better with increasing extrusion ratio. This can be attributed to that the increase of extrusion ratio can result

in more uniform exit temperature distribution in the extrusion process [15]. So, larger extrusion ratio is useful for obtaining the pipe with finer and more uniform grain in a practical extrusion process.

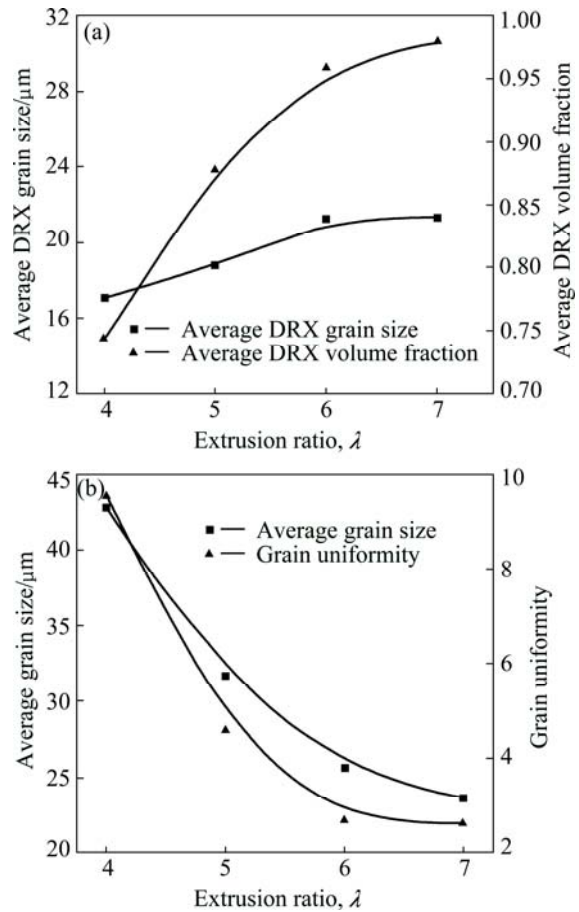


Fig. 15 Effect of extrusion ratio on DRX behavior in large-scale thick-walled Inconel 625 pipe extruded in stable stage: (a) Average DRX grain size and average DRX volume fraction; (b) Average grain size and grain uniformity

4.2.4 Friction coefficient

As shown in Fig. 16(a), larger friction coefficient can induce higher average DRX volume fraction and larger average DRX grain size. This is because larger friction coefficient can induce more friction heat, which can promote the occurrence of DRX and increase the DRX grain size.

Figure 16(b) shows the effect of friction coefficient on the average grain size and grain uniformity of the pipe. It can be seen that larger friction coefficient can lead to a slight decrease of average grain size of the pipes. In addition, with the increase of friction coefficient, the grain uniformity is firstly improved and then deteriorated. This phenomenon can be explained by the fact that the exit temperature uniformity in the pipe extrusion process firstly becomes better and then goes worse with the increase of friction coefficient [15].

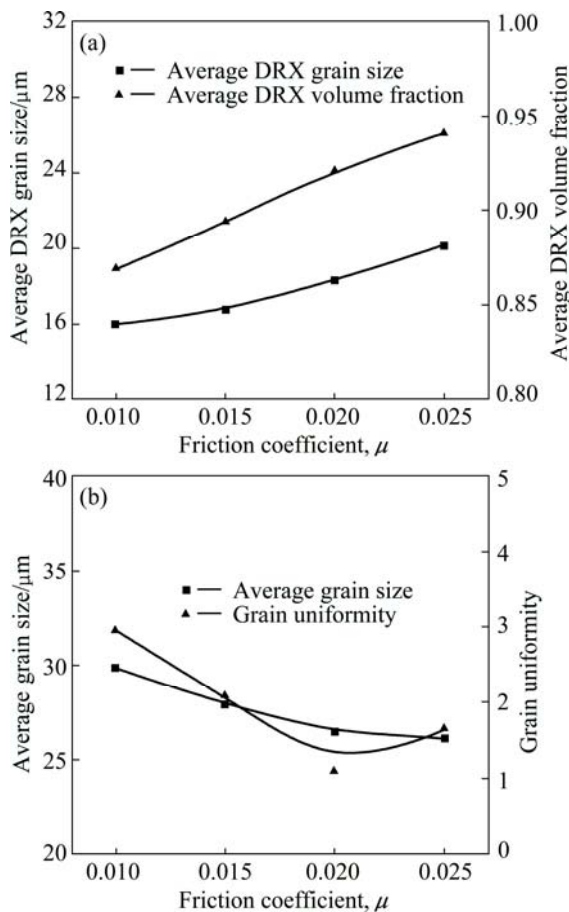


Fig. 16 Effect of friction coefficient on DRX behavior in large-scale thick-walled Inconel 625 pipe extruded in stable stage: (a) Average DRX grain size and average DRX volume fraction; (b) Average grain size and grain uniformity

5 Conclusions

1) The thermal-mechanical and micro-macro coupled finite element model, which can precisely predict the dynamical recrystallization behavior during the hot extrusion process of large-scale thick-walled Inconel 625 pipe, was developed by encoding the DRX evolution model of Inconel 625 alloy into the DEFORM-2D platform.

2) In the extrusion without remnant material process of large-scale thick-walled Inconel 625 pipe, the coarse grains are produced at the tail of the extruded pipe due to smaller deformation degree and lower deformation temperature. The grain size of the pipe extruded in the stable stage gradually increases from head to tail due to continuously decreasing DRX degree caused by continuously decreasing deformation temperature.

3) With the increase of initial billet temperature, the average grain size of the pipe extruded in stable stage firstly becomes smaller and then gets larger. Larger extrusion ratio can result in smaller grain size. The

extrusion speed and friction coefficient have slight effect on the grain size of the pipe.

4) With the increase of initial billet temperature, extrusion speed and friction coefficient, the grain uniformity of the pipe extruded in stable stage first becomes better and then goes worse. The larger extrusion ratio can result in more uniform grain distribution.

References

- [1] SHANKAR V, BHANU SANKARA RAO K, MANNAN S L. Microstructure and mechanical properties of Inconel 625 superalloy [J]. *Journal of Nuclear Material*, 2001, 288: 222–232.
- [2] SANJAY K R, ANISH K, SHANKAR V, JAYAKUMAR T, BHANU SAVKARA R K, BALDEV R. Characterization of microstructures in Inconel 625 using X-ray diffraction peak broadening and lattice parameter measurements [J]. *Scripta Materialia*, 2004, 51: 59–63.
- [3] SINGH J B, VERMA A, PAUL B. Failure of alloy 625 tube stub ends—Effect of primary nitrides [J]. *Engineering Failure Analysis*, 2013, 32: 236–247.
- [4] LI De-fu, GUO Qing-miao, GUO Sheng-li. The microstructure evolution and nucleation mechanisms of dynamic recrystallization in hot-deformed Inconel 625 super alloy [J]. *Materials and Design*, 2011, 32: 696–705.
- [5] GUO Qing-miao, LI De-fu, GUO Sheng-li. The effect of deformation temperature on the microstructure evolution of Inconel 625 superalloy [J]. *Journal of Nuclear Materials*, 2011, 414: 440–450.
- [6] WU Zhi-gang, LI De-fu, GUO Sheng-li. Dynamic recrystallization models of GH 625 Ni-based superalloy [J]. *Rare Metal Materials and Engineering*, 2012, 41(2): 235–240. (in Chinese)
- [7] LOPEZ B, URCOLA J J. Hot deformation characteristics of Inconel 625 [J]. *Materials Science and Technology*, 1996, 12: 673–678.
- [8] PENG Hai-jian, LI De-fu, GUO Qing-miao. Processing map and tube hot extrusion of GH 690 alloy [J]. *Chinese Journal of Rare Metals*, 2012, 36(2): 184–190. (in Chinese)
- [9] WANG Huai-liu. Study on hot extrusion process for GH 690 alloy [J]. *Special Steel Technology*, 2008, 14(51): 31–34. (in Chinese)
- [10] GUO Qing-miao, LI Hai-tao, LI De-fu. Hot extrusion moulding process and microstructure evolution of GH 625 superalloy tubes [J]. *China Journal of Rare Metals*, 2011, 35(5): 654–689. (in Chinese)
- [11] LIU Chen-ze, LIU Feng, HUANG Lan. Effect of hot extrusion and heat treatment on microstructure of nickel-base superalloy [J]. *Transactions of Nonferrous Metals Society of China*, 2014, 24(8): 2544–2553.
- [12] GUO Liang-gang, DONG Ke-ke, ZHANG Bao-jun. Dynamic recrystallization rules in needle piercing extrusion for AISI304 stainless steel pipe [J]. *Transactions of Nonferrous Metals Society of China*, 2012, 22(S2): s519–s527.
- [13] HE Qing-qiang, SUN Jia, YAN Cheng-xin. Thermo-mechanical modeling and simulation of microstructure evolution in multi-pass H-shape rolling [J]. *Finite Elements in Analysis and Design*, 2013, 76: 13–20.
- [14] ZHU S, YANG H, GUO L G, GU R J. Investigation of deformation degree and initial forming temperature dependences of microstructure in hot ring rolling of TA15 titanium alloy by multi-scale simulations [J]. *Computational Materials Science*, 2012, 6: 221–229.
- [15] DANG Li, YANG He, GUO Liang-gang, ZHENG Wen-da. Study on exit temperature evolution during extrusion for large-scale thick-walled Inconel 625 pipe by FE simulation [J]. *The International*

- Journal of Advanced Manufacturing Technology, 2015, 76: 1421–1435.
- [16] YAN Shi-cai, CHENG Ming, ZHANG Shi-hong. High temperature high speed hot deformation behavior of Inconel alloy 625 [J]. Chinese Journal of Materials Research, 2010, 24(3): 239–244. (in Chinese)
- [17] DAMODARAN D, SHIVPURI R. Effect of glass lubricant behavior on the surface quality of extrudates in glass-lubricated hot extrusion [J]. CIRP Annals — Manufacturing Technology, 1997, 46(1): 179–182.
- [18] HANSSON S, JANSSON T. Sensitivity analysis of a finite element model for the simulation of stainless steel tube extrusion [J]. Journal of Materials Processing Technology, 2010, 210: 1386–1396.
- [19] HANSSON S, FISK M. Simulations and measurements of combined induction heating and extrusion processes [J]. Finite Elements in Analysis and Design, 2010, 46: 905–915.

Inconel 625 大型厚壁管挤压动态再结晶演化规律仿真

党利¹, 杨合¹, 郭良刚¹, 石磊¹, 张君², 郑文达²

1. 西北工业大学 凝固技术国家重点实验室, 西安 710072;
2. 中国重型机械研究院有限公司, 西安 710032

摘要: 基于 DEFORM-2D 有限元平台, 建立能准确预测 Inconel 625 大型厚壁管挤压过程宏、微观变形行为的有限元模型。揭示关键挤压参数对挤压管动态再结晶平均晶粒尺寸及晶粒分布均匀性的影响规律。研究表明, 随着坯料初始温度、挤压速度和摩擦因数的增加, 管材晶粒分布均匀性呈先增加后降低的趋势; 增大挤压比能提高管材组织均匀性; 随着坯料初始温度的升高, 管材平均晶粒尺寸呈先减小后增大的趋势; 挤压比的增大能显著减小管材平均晶粒尺寸; 挤压速度和摩擦因数对管材平均晶粒尺寸的影响不明显。

关键词: Inconel 625 合金; 大型厚壁管; 挤压; 动态再结晶; 晶粒尺寸; 晶粒分布均匀性

(Edited by Wei-ping CHEN)